

UV light-triggered unpacking of DNA to enhance gene transfection of azobenzene-containing polycations†

Cite this: *J. Mater. Chem. B*, 2014, 2, 3868

Yongmao Li, Jianhai Yang, Liang Sun, Wei Wang and Wenguang Liu*

This study demonstrates a strategy to enhance gene delivery *via* photoregulated gene unpacking from its vector. Photoresponsive polycationic vectors composed of a middle azobenzene moiety and two terminal blocks of poly[2-(dimethylamino)ethyl methacrylate], termed as Azo-PDMAEMA, are synthesized using a difunctional azobenzene-based initiator *via* atomic transfer radiator polymerization (ATRP). The Azo-PDMAEMA exhibits *trans* to *cis* isomerization under alternate Vis-UV irradiation, and is capable of condensing plasmid DNA into nanocomplexes. Hydrophobic azobenzene groups in the cationic polymers are shown to enhance the interaction of complexes with the cell membrane, thus improving cell uptake and transfection efficiency. Increased gene expression in COS-7 cells, HepG-2 cells and CHO-K1 cells is achieved after UV irradiation due to UV-triggered intracellular gene unpacking. Time-resolved fluorescence assays further indicate that the *trans* to *cis* photoisomerization of Azo-PDMAEMA induces less compacted complexes, contributing to more exposure of genes for transcription.

Received 21st February 2014
Accepted 11th April 2014

DOI: 10.1039/c4tb00294f

www.rsc.org/MaterialsB

1. Introduction

Gene therapy has offered promising novel therapeutic approaches to fighting cancers and facilitating tissue repair or reconstruction in regenerative medicine. Its success is fundamentally dependent on the development of effective and safe gene delivery systems.^{1,2} Nonviral vectors, in particular cationic polymers, have been shown to be potential alternatives to viral vectors due to biosafety, design flexibility and easy scale-up.^{3–5} However, cationic polymers with positive charges condense DNA so tightly that the packed gene becomes increasingly difficult to dissociate from its carrier, seriously limiting the ultimate gene transfection.⁶ In order to promote gene liberation, new types of smart polymer vectors have been designed by incorporating environmental stimuli properties into polycation.⁷ These polymers are capable of responding to micro-environmental changes such as pH, temperature, light, magnetic field, enzyme and redox by varying macromolecular conformation.^{8–13}

Among these stimuli, light is especially appealing because it is clean energy and can be manipulated remotely, precisely and rapidly. Photosensitizers were reportedly used to destabilize the membrane of endocytic vesicles under light irradiation.^{14,15} Although the transfection efficiency could be improved by light

stimulation, most photosensitizers are highly toxic.¹⁶ Transfection using photocleavable polycationic gene carriers without any additive offers a promising way to solve this dilemma. UV light irradiation could lead to photochemical decomposition or cleavage; as a result, the condensed gene was released, resulting in a high level of DNA-transcription recovery *in vitro*.¹⁷ Previous work showed that the photoactivated *trans* to *cis* isomerization of azobenzene-cationic lipid could be exploited to destabilize the vesicle membrane, which accelerated the escape of gene from endosome and thus increased gene transfection in COS-1 cells.¹⁸

Recently, more studies have just focused on photoregulated drug delivery through azobenzene-modified mesostructured silica.¹⁹ Alternating UV and visible light irradiation led to the variation in the molecular size of azobenzene molecules attached to the pore interior accompanied by dynamic wagging azobenzene, thereby enabling controlled release of the entrapped drug.²⁰ During transition from *trans* to *cis* form, not only the molecular size becomes smaller, but also the substitutes on adjacent azobenzene groups move away from each other, leading to the enlargement of neighboring space of the intermolecule.²¹ Based on this principle, we hypothesize that if the azobenzene is incorporated into a cationic polymer, the obtained polycation-azobenzene is used to condense DNA into nanocomplexes, which are then subjected to UV light illumination. It is theoretically possible that along with *trans* to *cis* isomerization, the adjacent azobenzene groups surrounding the packed DNA move apart, which will result in the loosening or dissociation of genes, consequently improving transfection efficiency. Motivated by designing and fabricating a potent gene

School of Materials Science and Engineering, Tianjin Key Laboratory of Composite and Functional Materials, Tianjin University, Tianjin 300072, PR China. E-mail: wgliu@tju.edu.cn; Fax: +86 22 27402487; Tel: +86 22 27402487

† Electronic supplementary information (ESI) available. See DOI: 10.1039/c4tb00294f

delivery system applicable to delivering a variety of cell lines, we will synthesize a photoresponsive polycationic vector by atomic transfer radical polymerization of 2-(dimethylamino)ethyl methacrylate using a difunctional azobenzene-based initiator. It is anticipated that the enhanced cellular uptake of polyplexes as well as UV light-tuned gene unpacking could be achieved in this photoresponsive vector. The physicochemical properties of photoresponsive polycation/DNA nanocomplexes will be investigated and *in vitro* gene transfection of typical COS-7, HepG-2 and CHO-K1 cell lines under UV irradiation conditions will be evaluated.

2. Experimental

2.1. Synthesis of azobenzene-based initiator

The azobenzene-based initiator was prepared by condensation of 4,4'-diaminoazobenzene and 2-bromoisobutyryl bromide in THF, using triethylamine (TEA) as a acid scavenger. In brief, 4,4'-diaminoazobenzene (255 mg, 1.2 mmol) was dissolved in 20 ml of anhydrous THF in a 50 ml flask, to which triethylamine (670 μ l, 4.8 mmol) was added. The solution was stirred in an ice bath, and 2-bromoisobutyryl bromide (600 μ l, 4.8 mmol) in 10 ml dry THF was added dropwise over a period of 1 h under a nitrogen atmosphere; the mixture was then stirred at room temperature for 24 h. After the reaction was accomplished, the reaction mixture was filtered *via* vacuum filtration to remove the precipitate formed, and the tetrahydrofuran was removed by rotary evaporation. The obtained crude product was redissolved in a solution of chloroform and extracted with aqueous sodium bicarbonate solution. The extracted product was washed with water several times, dried with anhydrous magnesium sulphate, and then the residual solvent was removed *in vacuo*. Finally the solid product was purified by recrystallization from ethanol and a yellow powder was obtained.

2.2. Synthesis of azobenzene-containing PDMAEMA

To synthesize the azobenzene-containing PDMAEMA, CuCl (0.05 mmol, 5 mg) dissolved in 5 ml DMSO was placed in a clean, dry Schlenk flask equipped with a magnetic stir bar, and degassed *via* three freeze-thaw cycles. Then PMDETA (0.05 mmol, 11 μ l), the above synthesized initiator (0.025 mmol, 12.8 mg) and DMAEMA (3.75 mmol, 635 μ l) dissolved in 3 ml DMSO were added using a syringe under nitrogen and the reaction mixture was degassed *via* another three freeze-thaw cycles. The reaction was allowed at room temperature for 24 h under stirring. After that, the mixture was dialyzed against distilled water for 5 days to remove the impurities and unreacted monomers. Finally the product (termed as Azo-PDMAEMA₁₅₀) was collected by lyophilization. In the same manner, Azo-PDMAEMA₁₀₀ was also synthesized. PDMAEMA₁₅₀ was prepared *via* ATRP using DEDBA as an initiator according to the above protocol.

2.3. Preparation of polymer/pDNA complexes

PDMAEMA₁₅₀ and Azo-PDMAEMA were separately dissolved in PBS (pH = 7.4). The complexes at various weight ratios were

then formulated by adding the polymer aqueous solution with a desired concentration to an equal volume of pDNA, vortexed for 10 s, and incubated for 30 min at room temperature. In this study, the complexation ratio was expressed as the weight ratio of polymer/pDNA.

2.4. Complex stability in the presence of heparin

To test the stability of complexes, the complex solutions were incubated with increasing concentrations of heparin (0.6–2.2 IU per μ g DNA) for 10 min at room temperature and analyzed by agarose gel electrophoresis. The image was captured through Bio-Imaging systems (UVP).

2.5. Cytotoxicity assay

In vitro cytotoxicity of polymer/pDNA complexes with varied complexation ratios was evaluated according to the previously reported method.²²

To evaluate the UV light induced-cytotoxicity, the cells were irradiated under an UV lamp (365 nm, 2 mW cm⁻²) for 0–900 s. Both UV-irradiated cells and non-irradiated cells were further cultured for 24 h. Then the cell viability was assayed according to the previous protocol.²²

2.6. *In vitro* transfection and luciferase assay

Cells were seeded at a density of 5×10^4 cells per well onto 24-well plates and incubated at 37 °C until they reached about 80% confluence. Before transfection, the medium in each well was replaced with 450 μ l of fresh medium containing 10% FBS, and 50 μ l complexes with different weight ratios were added into each well (1 μ g DNA per well). The culture plates were divided into two groups. Group I was continuously incubated for 24 h. For group II, after incubating for 20 h, the cells were irradiated for 10 min under an UV lamp (365 nm, 2 mW cm⁻²), and then incubated for another 4 h. Each group was replaced with 500 μ l of fresh culture medium plus 10% FBS, and the cells were further incubated for 24 h. The luminescence of each sample was measured according to our previous study.²³ 25 kDa branched polyethylenimine (PEI25k) was used as a positive control at a weight ratio of 2 : 1. All the experiments were carried out in triplicate.

To further evaluate the transfection efficiency of Azo-PDMAEMA, pEGFP-C1 plasmid transfection in HepG-2 cells was performed. Cells were seeded in 12-well plates at a density of 2×10^5 cells per well for 24 h for transfection and the medium was refreshed with 900 μ l complete medium. 100 μ l of complex solution containing 2 μ g DNA at the optimal weight ratios was added to each well. The transfection was performed as described previously.²⁴ Finally the transfected cells were observed using an inverted fluorescence microscope (Olympus, 1X-51) or measured by flow cytometry (FACS Calibur, BD, USA). The PEI25k/DNA complex with a weight ratio of 2 : 1 served as a positive control.

2.7. Determination of cellular internalization

HepG-2 cells were seeded into a 6-well plate at a density of 4×10^5 cells per well and incubated for 24 h. Then the medium was

replaced with 1800 μl DMEM containing 10% FBS without antibiotics. The pGL3-control was labeled with YOYO-1 iodide according to the following process: 1 mmol l^{-1} YOYO-1 was diluted 100 times with PBS. Then 1 μg of DNA was labeled using 1 μl YOYO-1 dilution and incubated for 2 h in the dark. Preparation of vector/YOYO-1-pDNA complexes was performed as described above. 200 μl complexes containing 6 μg of labeled pDNA were added to each well and the plate was further incubated for 4 h. After that, the cells were washed three times using PBS to remove the uninternalized complexes and culture medium, and then trypsinized and harvested in PBS. The fluorescence intensity of the cells was measured by flow cytometry (FACS Calibur, BD, USA).

2.8. Statistical analysis

Group data are expressed as mean \pm SD. For transfection results, the two population student's *t*-test was used to determine whether data groups differed significantly from each other. Statistical significance was defined as having $P^* < 0.05$.

3. Results and discussion

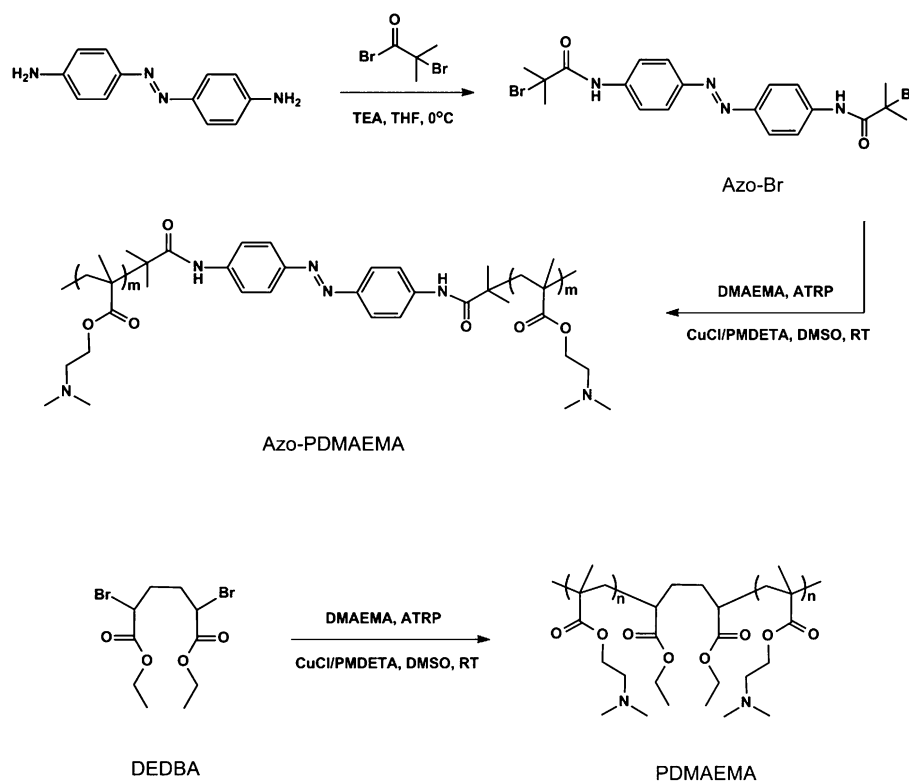
3.1. Characterization of azobenzene-based initiator and azobenzene-containing PDMAEMA

The synthesis of Azo-PDMAEMA and PDMAEMA is illustrated in Scheme 1. The difunctional azobenzene-based initiator was first prepared, and used to initiate ATRP of DMAEMA incorporating azobenzene groups in the middle of the polymer chain.

Fig. 1 exhibits the ^1H NMR spectra of the azobenzene-based initiator (A) and azobenzene-containing polymers (B). As shown in Fig. 1A, the peak located at a chemical shift of $\delta = 1.8$ ppm is associated with the methyl protons (**d**, $-\text{C}(\text{CH}_3)_2-\text{Br}$) of 2-bromoisobutryl groups.²⁵ The signal at $\delta = 7.9$ ppm is attributable to the amido protons (**c**, $-\text{NH}-\text{CO}-$).²⁶ The characteristic signals corresponding to the phenyl protons of the azobenzene group are observed at $\delta = 7.6$ ppm and $\delta = 6.9$ ppm, respectively.²⁷ In Fig. 1B, there appear feature signals of DMAEMA at $\delta = 2.2$, $\delta = 2.6$, $\delta = 4.0$, $\delta = 1.8$, and $\delta = 0.8$ corresponding to methyl protons (**1**, $-\text{N}-(\text{CH}_3)_2$), methylene protons (**2**, $-\text{CH}_2-\text{N}-$), methylene protons (**3**, $-\text{O}-\text{CH}_2-$), methylene protons (**5**, $-\text{CH}_2-\text{C}-$) and methyl protons (**6**, $-\text{C}-\text{CH}_3$), respectively.²⁸ The results manifest that the difunctional initiator and Azo-PDMAEMA have been successfully prepared.

Table S1† shows the number average molecular weights (M_n) of polymers. The molecular distribution is in the 1.16–1.24 range, indicating that the polymerization of DMAEMA initiated by the azobenzene-based difunctional initiator was well-controlled.

The *trans* to *cis* photoisomerization of the azobenzene-based initiator and Azo-PDMAEMA was inspected by UV-Vis absorption spectra under ultraviolet light (365 nm) irradiation. The UV-Vis spectra of the azobenzene-based initiator in THF recorded at different irradiation times are given in Fig. 2A. During the illumination, the absorption maximum at about 420 nm corresponding to the $\pi-\pi^*$ transition of *trans*-azobenzene is decreased with time. This spectral change is attributed to the transition from the *trans* form to the *cis* form. A similar behavior



Scheme 1 Synthetic procedure of an azobenzene-based initiator, azobenzene-containing PDMAEMA and PDMAEMA.

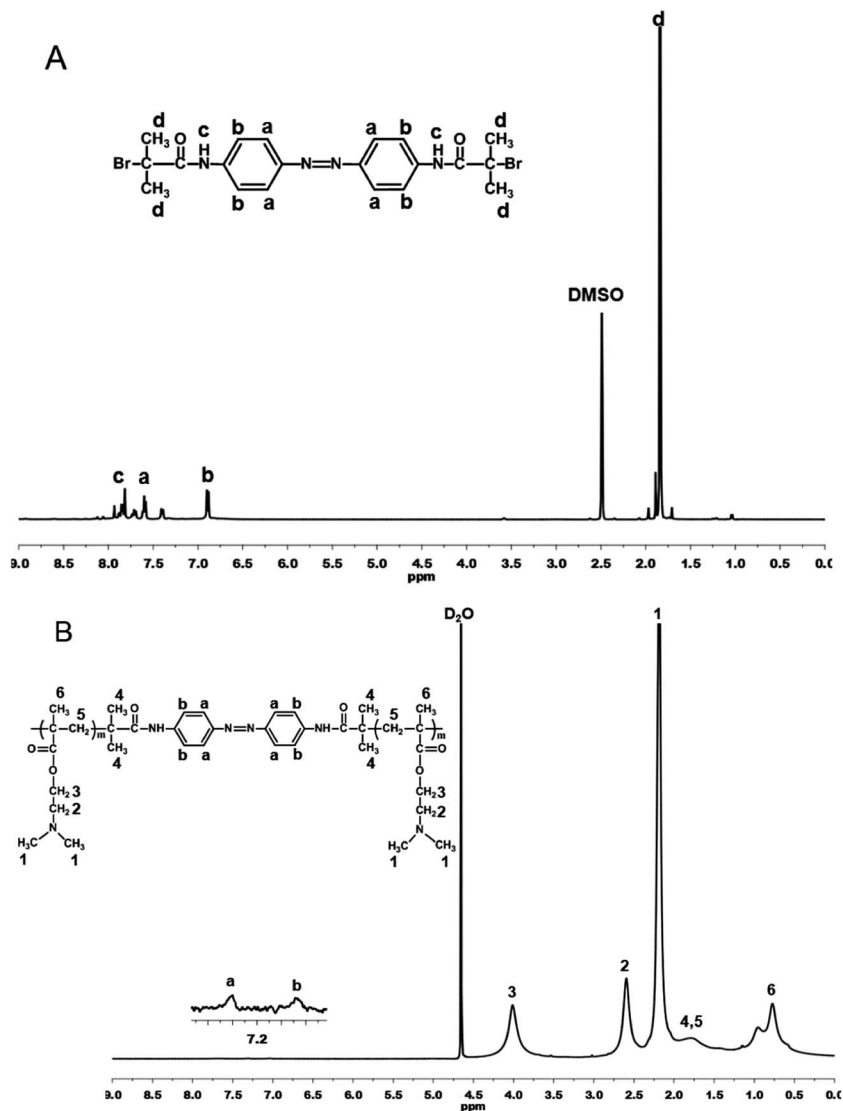


Fig. 1 ^1H NMR spectra of (A) azobenzene-based initiator in DMSO-d_6 and (B) Azo-PDMAEMA $_{150}$ in D_2O .

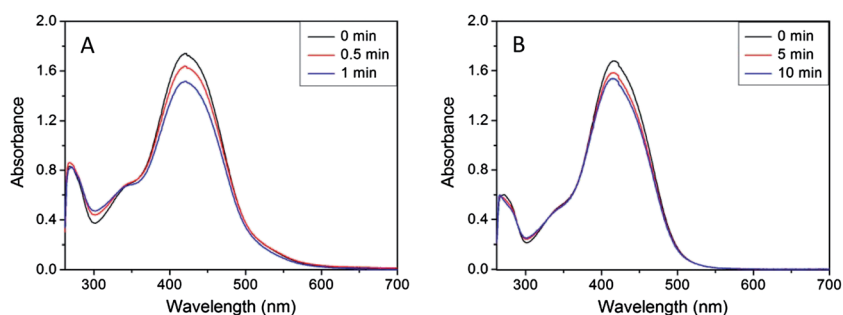


Fig. 2 UV-Vis spectral change of azobenzene-based initiator in THF (A) and Azo-PDMAEMA $_{150}$ in water (B) after irradiation with a UV lamp (365 nm) for different times.

is observed upon UV irradiation of Azo-PDMAEMA $_{150}$ (Fig. 2B). Nevertheless, the *trans-cis* isomerization rate of Azo-PDMAEMA $_{150}$ is lower compared with that of the azo-initiator due to the steric hindrance of polymer chains. Overall, these

results are consistent with the previously reported data²⁹ and clearly demonstrate that azobenzene-incorporated PDMAEMA displays a typical transition from the *trans* form to the *cis* form by the photochemical procedure.

3.2. Physicochemical properties of Azo-PDMAEMA/pDNA complexes

The ability of the azobenzene-containing cationic polymer to condense DNA is essential for achieving efficient transfection. Fig. S1† displays the agarose gel electrophoresis patterns of the Azo-PDMAEMA/pDNA complexes at various weight ratios ranging from 0.2 to 1.6. The migrating free DNA is gradually retarded with increasing complex ratio. A complete retardation

of complexes is observed for Azo-PDMAEMA₁₅₀, Azo-PDMAEMA₁₀₀ and PDMAEMA₁₅₀ at ratios of 0.4, 0.6, and 0.4, respectively. Compared with the other two vectors, Azo-PDMAEMA₁₀₀ has a relatively higher critical complexation ratio, which is attributed to the less positive charges in molecular chains.

To investigate the effect of UV irradiation on Azo-PDMAEMA-induced DNA condensation, agarose gel electrophoresis was

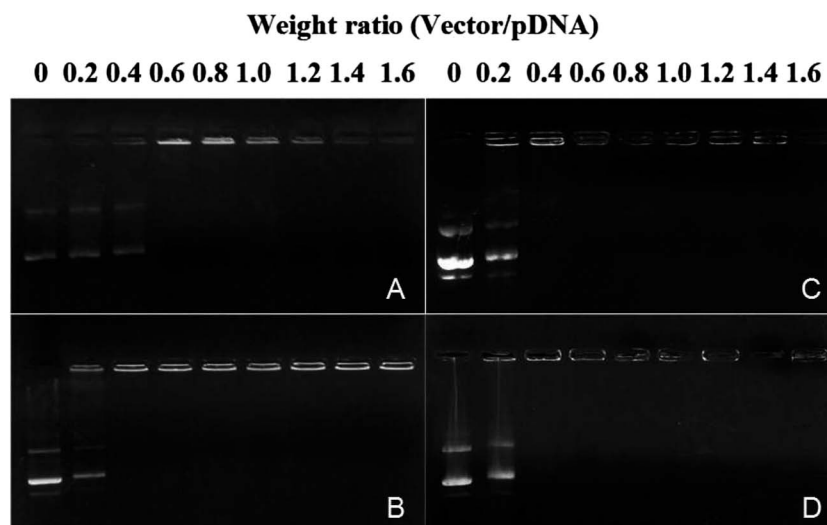


Fig. 3 Agarose gel electrophoresis retardation assay of vectors/pDNA complexes at different weight ratios: Azo-PDMAEMA₁₅₀/pDNA complexes irradiated with UV light before running (A), Azo-PDMAEMA₁₅₀/pDNA complexes without UV light irradiation before running (B), PDMAEMA₁₅₀/pDNA complexes irradiated with UV light before running (C), PDMAEMA₁₅₀/pDNA complexes without UV light irradiation before running (D).

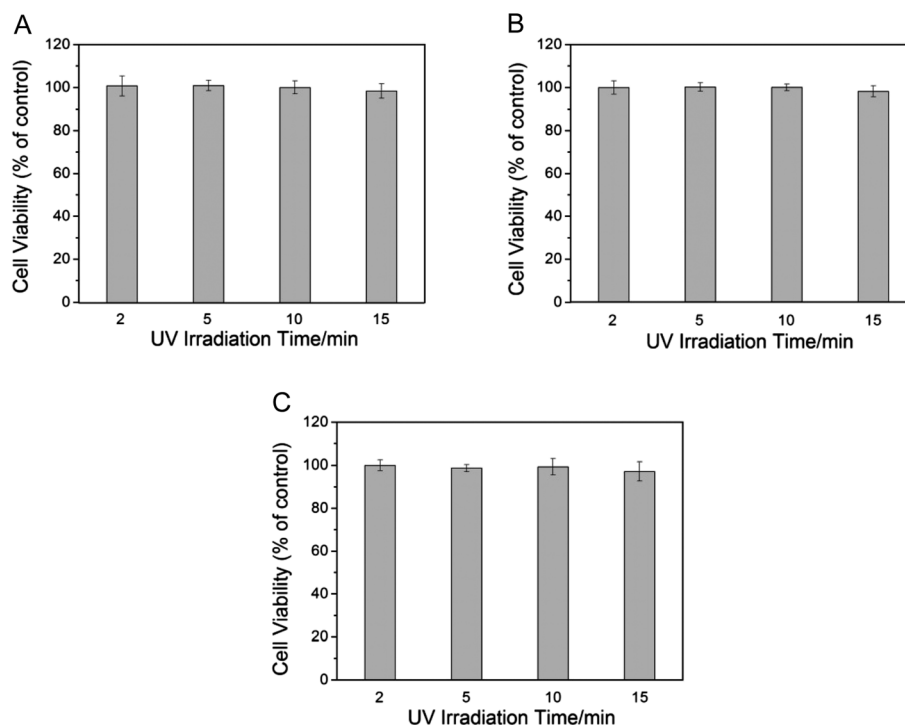


Fig. 4 Cytotoxicity testing results from a MTT assay in (A) COS-7 cells, (B) HepG-2 cells and (C) CHO-K1 cells after UV irradiation for different time periods. The values represent percentage of cell viability.

performed by UV light treatment of polyplexes. It is found that after complexes are irradiated by UV light for 10 min, the complexation ratio at which the Azo-PDMAEMA₁₅₀/pDNA complex is entirely retarded increases to 0.6 (Fig. 3A), higher than that under normal conditions (Fig. 3B). While, no different electrophoresis retardation band is observed for PDMAEMA₁₅₀/pDNA complexes with or without UV light illumination (Fig. 3C and D). The above comparative results suggest that UV light-triggered *trans-cis* transition of azobenzene results in loosening or unpacking of complexes to some extent. In contrast, there is no change in the configuration of macromolecular chains in light insensitive PDMAEMA₁₅₀ under conditions of UV light stimulation.

TEM was used to examine the morphology of Azo-PDMAEMA₁₀₀/pDNA, Azo-PDMAEMA₁₅₀/pDNA and PDMAEMA₁₅₀/pDNA complexes formed at the selected ratio of 8 : 1. All of the polymers can condense DNA into nanospheres with similar diameters about 50 nm (Fig. S2†). Fig. S3A† shows that the hydrodynamic sizes of Azo-PDMAEMA/pDNA complexes and PDMAEMA/pDNA complexes at varied ratios exhibit a declining trend with an increment in the complexation ratio, due to more compact condensation of DNA at higher positive charge ratios. Zeta potentials are enhanced with an

increase of complexation ratio up to 10, and maintained at 16–18 mV (Fig. S3B†). The stability of the complexes against exchange reactions with heparin sodium was examined with gel electrophoresis (Fig. S4†). For PDMAEMA₁₅₀, Azo-PDMAEMA₁₀₀ and Azo-PDMAEMA₁₅₀, the threshold concentrations of heparin sodium at which the dissociation of complexes occurs are 1.0 IU, 1.8 IU and 2.0 IU, respectively. The result suggests that the complexes formulated by azobenzene-containing cationic polymers are more stable than PDMAEMA/DNA polyplexes. Thus, it is rational to deduce that the presence of benzyl groups plays an important role in preserving the stability of azobenzene-based cationic polymer/pDNA polyplexes *via* hydrophobic forces.²⁶

The vulnerability of pDNA toward nuclease is another obstacle for the transfection. In order to substantiate the protection of pDNA provided by the vectors, DNase I was used to treat the formulated complexes. From the gel electrophoresis patterns (Fig. S5†), we can see that Azo-PDMAEMA₁₅₀ could protect the condensed pDNA even after 2 h of incubation with DNase I, while the naked pDNA was found to be completely digested by the enzyme within only 5 min of treatment. In contrast, PDMAEMA₁₅₀ shows poorer DNA protection than Azo-PDMAEMA₁₅₀. The results suggest that Azo-PDMAEMA₁₅₀ has a

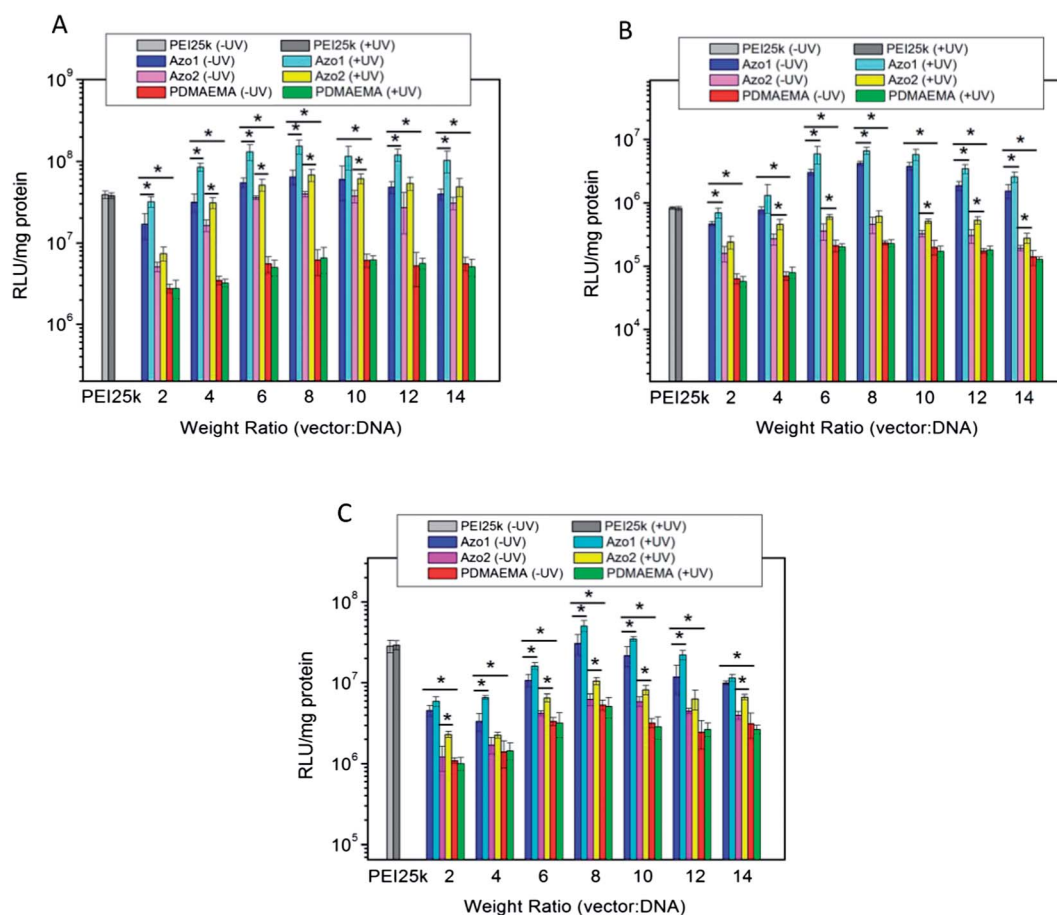


Fig. 5 *In vitro* gene transfection efficiency of the three kinds of cationic polymers/pDNA complexes in comparison with that of PEI25k at various weight complexation ratios in COS-7 cells (A), HepG-2 cells (B) and CHO-K1 cells (C). Azo1: Azo-PDMAEMA₁₅₀, Azo2: Azo-PDMAEMA₁₀₀, PDMAEMA: PDMAEMA₁₅₀, -UV: without UV irradiation, +UV: UV irradiation.

better ability to protect the complexed pDNA from degradation by nucleases.

3.3. Cytotoxicity evaluation

To determine the appropriate time for UV irradiation, the effect of different exposure times on the cytotoxicity was investigated by conducting MTT assays in COS-7 cells, HepG-2 cells and CHO-K1 cells, respectively. Fig. 4 exhibits that for the above three cell lines, a period of less than 10 min of UV light exposure has almost no influence on the viability of cells (Fig. 4A–C). However, a slight decrease in cell viability is seen after 15 min of irradiation. Therefore, in the following transfection experiment, 10 min UV irradiation was selected for the three cells.

We also evaluated the cytotoxicity of cationic polymer/pDNA complexes with different complexation ratios against the above three cells in comparison with that of the PEI25k/pDNA complex at its optimal weight ratio of 2 : 1. Fig. S6† demonstrates that the cytotoxicity of all the vectors increases as the

complexation ratio is raised; moreover the three vectors exhibit similar cytotoxicity at the same complexation ratio. However, at the complexation ratios ranging from 2 to 8, the cytocompatibility of Azo-PDMAEMA₁₅₀/pDNA complexes is superior to that of the PEI25k/pDNA complex.

3.4. *In vitro* gene transfection

In this study, we first evaluated the effect of UV illumination on the transfection efficiency of three kinds of cationic polymer/pDNA complexes in COS-7 cells, HepG-2 cells and CHO-K1 cells. Two routes of UV irradiation and non-UV irradiation were applied to assess the cationic polymer-mediated gene transfection at various complexation ratios from 2 : 1 to 14 : 1 (Fig. 5). The results demonstrate that the transfection efficiency is increased firstly with the increment of complexation ratio, and at 8 : 1 ratio all of the three cationic polymers achieve the highest efficiency. At higher complexation ratios, the transfection level is decreased, which may be resulted from the

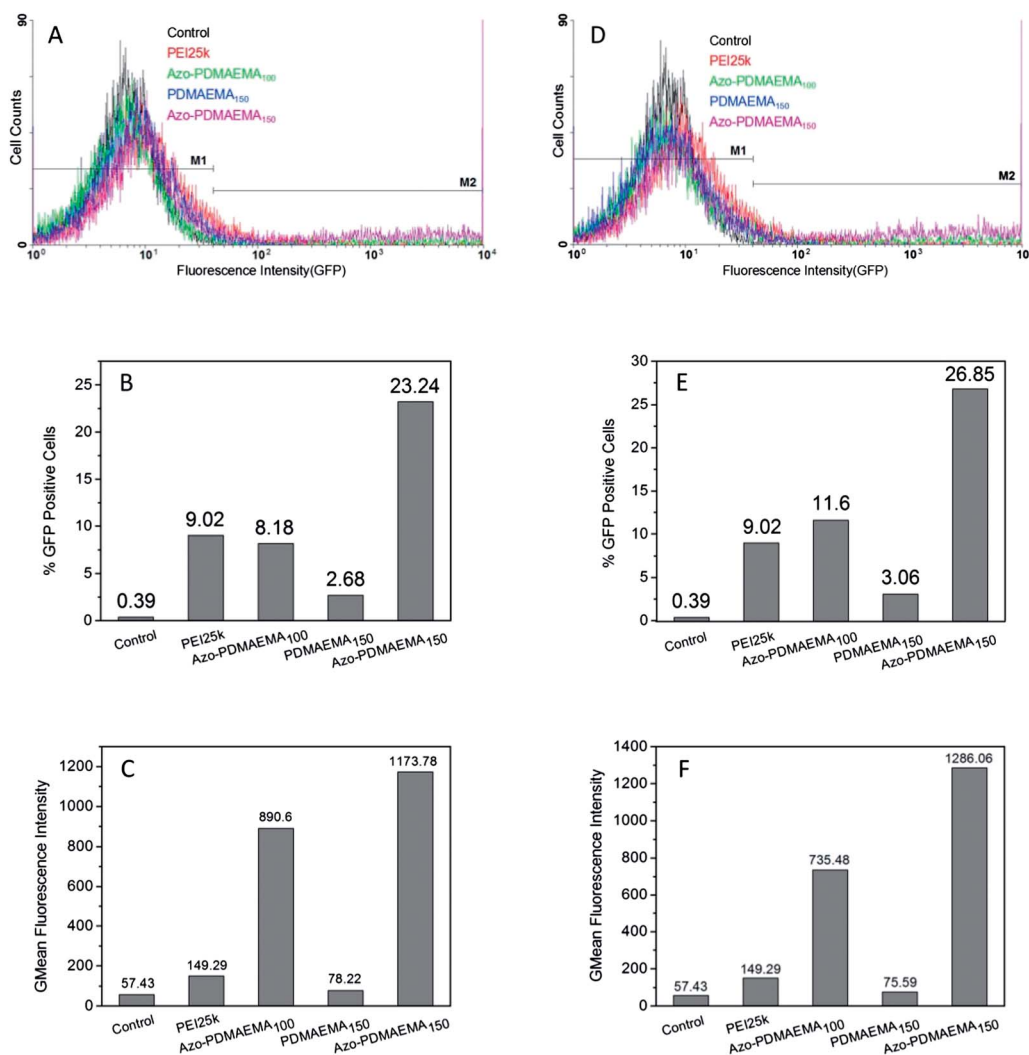


Fig. 6 Analysis results of the GFP expression mediated by three kinds of cationic polymers/pDNA complexes in HepG-2 cells using a flow cytometer. PEI25k/pDNA (2 : 1, w/w); Azo-PDMAEMA₁₅₀/pDNA (8 : 1, w/w); Azo-PDMAEMA₁₀₀/pDNA (8 : 1, w/w); PDMAEMA₁₅₀/pDNA (8 : 1, w/w). The analytical results of the transfected cells before UV irradiation (A–C) and after UV irradiation (D–F).

increased cytotoxicity of the vector. One important phenomenon is that all Azo-PDMAEMA polyplexes exhibit apparently higher transfection activities than PDMAEMA polyplexes in all cells. Among the three cationic polymers, Azo-PDMAEMA₁₅₀ displays the best transfection efficiency in all cell lines, which is comparable or superior to PEI25k in some cells. Although the transfection efficiency of Azo-PDMAEMA₁₀₀ is lower than that of Azo-PDMAEMA₁₅₀ due to the relatively lower positive surface charge on the former, it is still more effective than that of PDMAEMA₁₅₀. The maximal luciferase expression level mediated by Azo-PDMAEMA₁₅₀ in COS-7 cells, HepG-2 cells and CHO-K1 cells is 10.6, 18.9 and 6.8 times higher than that of PDMAEMA₁₅₀, respectively. In particular, such transfection enhancement attributed to the incorporation of hydrophobic azobenzene groups becomes more remarkable in HepG-2 cells.

Fig. 5 clearly shows that after application of UV irradiation, the photoresponsive Azo-PDMAEMA achieves a higher transfection level than that under normal culture conditions in three cell lines. An UV irradiation protocol contributes to 1.9–2.7 fold, 1.5–1.9 fold and 1.1–2 fold increase in transfection efficiency of COS-7 cells, HepG-2 cells and CHO-K1 cells infected with Azo-PDMAEMA₁₅₀/pDNA complexes, respectively. While for light insensitive PDMAEMA₁₅₀ and PEI25k, there is no significant difference in the transfection efficiencies in two routes. Thus, it is rational to consider that the increased transfection level under UV irradiation conditions is mainly from the *trans* to *cis* photoisomerization of the photoresponsive Azo-PDMAEMA, which induces formation of less compacted complexes, thus contributing to more exposure of genes for transcription.

To further evaluate the gene transfection of Azo-PDMAEMA, we assessed the expression of pEGFP in HepG-2 cells at an optimum weight ratio (Fig. S7†). The EGFP expression was also analyzed by flow cytometry (Fig. 6). It is noticeable that Azo-PDMAEMA achieves much higher EGFP expression than

PDMAEMA and PEI25k. Moreover, for Azo-PDMAEMA₁₅₀ and Azo-PDMAEMA₁₀₀, UV irradiation results in a further increase in EGFP expression. However for PDMAEMA₁₅₀, no obvious changes in EGFP expression are observed after UV irradiation. This result is consistent with the luciferase reporter system. The data analyses provided by flow cytometry also confirm the UV light stimulation effect. After transfection with Azo-PDMAEMA₁₅₀/pDNA and Azo-PDMAEMA₁₀₀/pDNA complexes, 23.24% and 8.18% cells are detected to express EGFP, respectively. Whereas the cells transfected by PDMAEMA₁₅₀/pDNA complexes only have 2.68% EGFP expressed, an indication that modification with hydrophobic azobenzene groups can significantly improve the gene transfection efficiency. After UV irradiation, 26.85%, 11.6% and 3.06% cells express EGFP mediated with Azo-PDMAEMA₁₅₀, Azo-PDMAEMA₁₀₀ and PDMAEMA₁₅₀, respectively. It seems that PDMAEMA in the absence of azobenzene leads to the increased gene expression too. But this change is marginal and insignificant. The average fluorescence intensity of all cells recorded by the flow cytometer also proves the remarkable transfection efficiency of Azo-PDMAEMA. Azo-PDMAEMA₁₅₀/pDNA complex-transfected cells exhibit about 15-fold higher fluorescence intensity than those with PDMAEMA₁₅₀/pDNA, 8 times higher than those transfected with PEI25k/pDNA complexes.

3.5. Mechanism underlying Azo-PDMAEMA-facilitated cellular uptake and intracellular unpacking of gene

Previous studies have shown that hydrophobic modifications can facilitate gene delivery due to the improved ability of polyplexes to fuse with the cell membrane and concomitantly increased cellular internalization.³⁰ In this study, the cellular uptake of the complexes was assayed by flow cytometry. Fig. 7 shows that the internalization rates of complexes formed by PEI25k and Azo-PDMAEMA₁₅₀ are 95.90% and 99.44%,

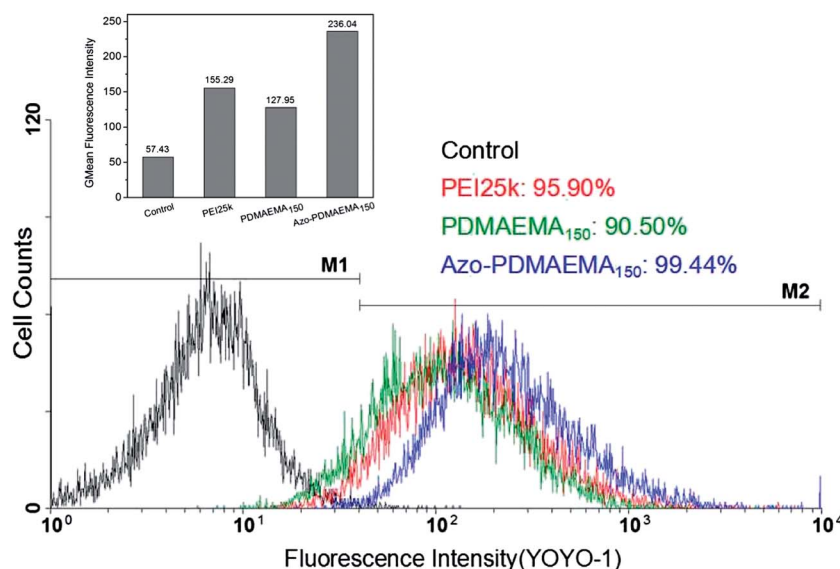


Fig. 7 Cellular internalization of complexes in HepG-2 cells analysed by a flow cytometer. PEI25k/pDNA (2 : 1, w/w); Azo-PDMAEMA₁₅₀/pDNA (8 : 1, w/w); PDMAEMA₁₅₀/pDNA (8 : 1, w/w).

respectively. By contrast, the PDMAEMA₁₅₀/pDNA complex displays poor cellular association with a 90.50% internalization rate, lower than that of Azo-PDMAEMA₁₅₀/DNA complexes. But the average fluorescence intensity is significantly different in that the intensity of Azo-PDMAEMA₁₅₀/DNA complexes is about 1.8-fold higher than that of PDMAEMA₁₅₀/DNA complexes, and 1.5-fold higher than that of PEI25k/pDNA complexes.

DPPC is a major component of cell membranes and DPPC has been widely used to characterize the cationic peptide, drug, and polymer induced membrane perturbation.³¹ Herein, the phase transition of DPPC induced by PDMAEMA₁₅₀ and Azo-PDMAEMA₁₅₀ was examined by DSC. As shown in Fig. S8,† the pure DPPC bilayer membrane undergoes gel to liquid crystalline transition at around 40.2 °C and the enthalpy is 22.6 J g⁻¹. Along with adding PDMAEMA₁₅₀, the enthalpy of phase transition associated with DPPC decreases to 14.1 J g⁻¹, evidencing that the cationic polymer vector leads to obvious destabilization of membranes. Notably, Azo-PDMAEMA₁₅₀ causes a very strong perturbation of DPPC bilayer membranes, resulting in a sharp

drop in the transition enthalpy from 22.6 J g⁻¹ to 8.9 J g⁻¹. The electrostatic interaction of DPPC head groups with other charged groups of cationic polymers is the major driving force for PDMAEMA₁₅₀-induced perturbation of DPPC.²⁸ But for Azo-PDMAEMA₁₅₀, electrostatic interaction may not be the only driving force. Hydrophobic interaction of azobenzene may also be involved in the perturbation of cell membranes. It has been proved that hydrophobic groups not only bind to the cell membrane surface, but also penetrate deeper into the hydrophobic core of the DPPC bilayer.^{32–34} Thus Azo-PDMAEMA is capable of disturbing the membrane to a greater extent thus facilitating cellular internalization and improving the transfection efficiency.

To explore the dynamic DNA condensation and decondensation, we recorded the fluorescence decay curves of EB/DNA complexes in PBS (pH = 7.4) in the presence of different amounts of cationic polymers with and without UV irradiation (Fig. S9†). One-exponential and two-exponential fluorescence decays of EB/DNA in the absence and presence of cationic

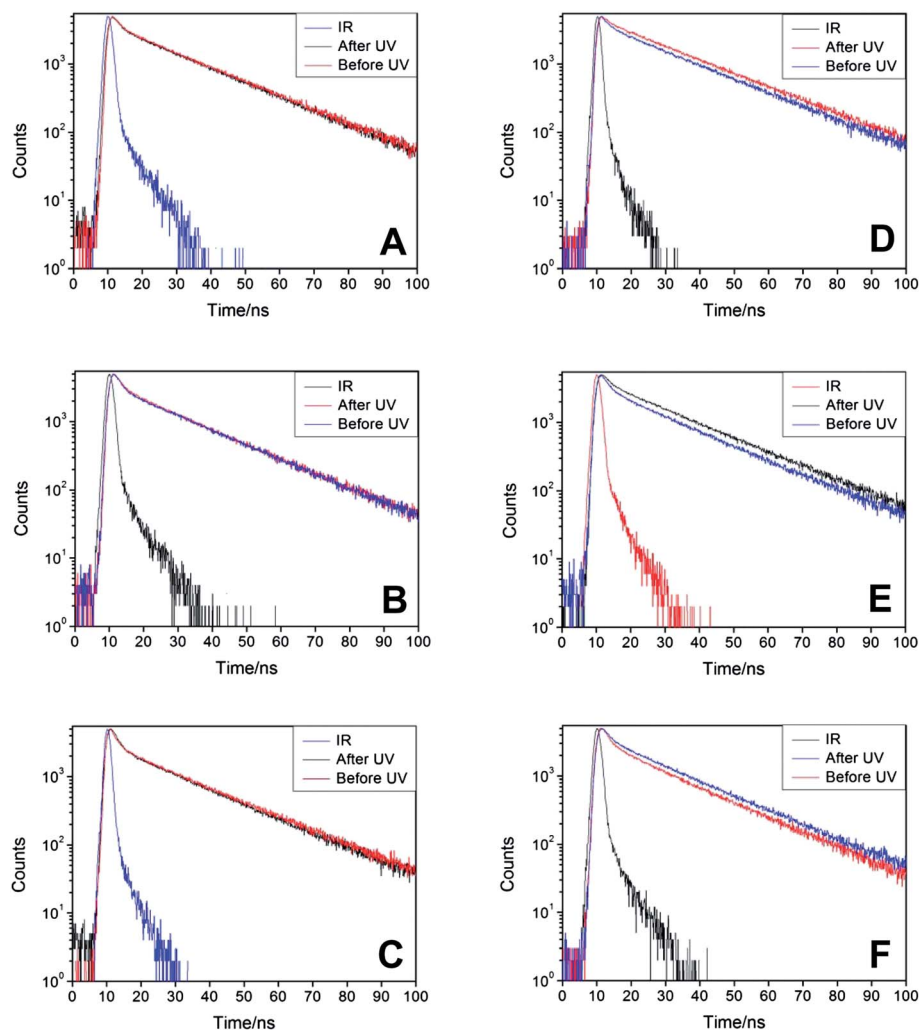


Fig. 8 The changes in the fluorescence decay curves after UV irradiation: PDMAEMA₁₅₀/EB/pDNA complexes at the weight ratio of 6 : 1 (A); PDMAEMA₁₅₀/EB/pDNA complexes at the weight ratio of 12 : 1 (B); PDMAEMA₁₅₀/EB/pDNA complexes at the weight ratio of 18 : 1 (C); Azo-PDMAEMA₁₅₀/EB/pDNA complexes at the weight ratio of 6 : 1 (D); Azo-PDMAEMA₁₅₀/EB/pDNA complexes at the weight ratio of 12 : 1 (E); Azo-PDMAEMA₁₅₀/EB/pDNA complexes at the weight ratio of 18 : 1 (F).

polymers are observed, respectively. With the increment of weight ratio, the fluorescence decay curve moves downward (Fig. S9†). For the PDMAEMA₁₅₀/EB/DNA systems, no obvious changes are observed in the fluorescence decay curves after UV irradiation. However the fluorescence decay curve moves upward when the Azo-PDMAEMA₁₅₀/EB/DNA complexes are irradiated with UV light (Fig. 8). The fluorescence decay curves are fitted with a two-exponential decay model. The obtained lifetimes and the relevant populations are listed in Tables S2 and S3.† The comparatively longer lifetime (τ_2) reflects the formation of the EB/DNA complex, and the shorter lifetime (τ_1) stems from the free EB.³⁵ EB gives only one single long-lived lifetime in the EB/DNA complex owing to the complete intercalation into DNA base-pairs. The addition of polymer vectors does not affect τ_1 and τ_2 values of the systems, but the populations of τ_1 and τ_2 vary. All the populations of τ_1 are increased with the increment of the polymer/DNA weight ratio, and those of τ_2 are accordingly decreased. The results imply that more intercalated EB probes are replaced by increased amounts of vectors, hinting polyplexes become more compact.

We also examined the effect of UV irradiation on the population of lifetime of photoresponsive Azo-PDMAEMA₁₅₀/EB/DNA and PDMAEMA₁₅₀/EB/DNA systems. To eliminate the influence of UV light itself, we subtracted the population of τ_1 after UV irradiation from that before UV irradiation to obtain the population difference of τ_1 , ΔP_1 . The ΔP_1 values of the photoresponsive Azo-PDMAEMA₁₅₀/EB/DNA system change from 11% to 14% (Table S3†), whereas that of the PDMAEMA₁₅₀/EB/DNA system is only in the range of -4% to 3% (Table S2†), irregular and much lower than that of the Azo-PDMAEMA₁₅₀/EB/DNA system. This significant difference of ΔP_1 suggests that after UV irradiation, the *trans*-to-*cis* isomerization of the

azobenzene alters conformation of cationic polymers, consequently contributing to the unpacking of the complexes. The complexes containing azobenzene moieties in their *trans* form are more compact than the same complexes with azobenzene adopting the *cis* form. Thus, UV light irradiation can promote the dissociation of DNA from the complexes, consequently improving gene expression. Based on the above analysis, we propose a mechanism underlying Azo-PDMAEMA-facilitated cellular internalization and intracellular unpacking of gene (Scheme 2).

4. Conclusions

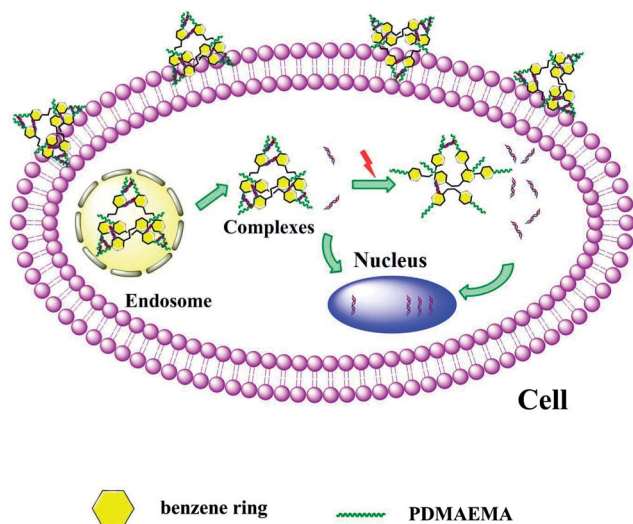
In summary, we have designed and fabricated photoresponsive azobenzene-centered polycationic vectors (Azo-PDMAEMA) for gene delivery *via* atomic transfer radical polymerization of 2-(dimethylamino)ethyl methacrylate initiated with difunctional initiator bearing azobenzene. The Azo-PDMAEMA demonstrated reversible *trans*-*cis* photoisomerization upon alternate irradiation with UV and visible light. Azobenzene in the midpoint of macromolecular chains was shown to contribute to an increase in gene transfection of multiple cell types due to the enhanced interaction with the cell membrane facilitated by hydrophobic fusion. A short-time of UV light illumination could trigger the dissociation of gene from polyplexes, thus further increasing transfection efficiency of multiple cells in the presence of serum.

Acknowledgements

The authors gratefully acknowledge the support for this work from the National Natural Science Foundation of China (Grants 51173129, 51325305) and National Science and Technology Major Project of China (Grants 2012ZX10004801-003-007, 2012AA022603).

References

- 1 I. M. Verma and N. Somia, *Nature*, 1997, **389**, 239.
- 2 R. J. Levy, S. A. Goldstein and J. Bonadio, *Adv. Drug Delivery Rev.*, 1998, **33**, 53.
- 3 T. Niidome and L. Huang, *Gene Ther.*, 2002, **9**, 1647.
- 4 S. Li and L. Huang, *Gene Ther.*, 2000, **7**, 31.
- 5 M. Thomas and A. M. Klivanov, *Appl. Microbiol. Biotechnol.*, 2003, **62**, 27.
- 6 D. W. Pack, A. S. Hoffman, S. Pun and P. S. Stayton, *Nat. Rev. Drug Discovery*, 2005, **4**, 581.
- 7 S. Dinçer, M. Türk and E. Pişkin, *Gene Ther.*, 2005, **12**, 139.
- 8 Z. Liu, M. Zheng, F. Meng and Z. Zhong, *Biomaterials*, 2011, **32**, 9109.
- 9 J. Yang, P. Zhang, L. Tang, P. Sun, W. Liu, P. Sun, A. Zuo and D. Liang, *Biomaterials*, 2010, **31**, 144.
- 10 N. Nishiyama, A. Iriyama, W. D. Jang, K. Miyata, K. Itaka, Y. Inoue, H. Takahashi, Y. Yanagi, Y. Tamaki, H. Koyama and K. Kataoka, *Nat. Mater.*, 2005, **4**, 934.
- 11 H. Wang, J. Yang, Y. Li, L. Sun and W. Liu, *J. Mater. Chem. B*, 2013, **1**, 43.



Scheme 2 The mechanism of the UV light stimuli-induced enhancement in gene transfection. Firstly the polyplexes are internalized into the cells *via* endocytosis and are trapped in endosomes. After endosomal escape, UV light irradiation is utilized, and the *trans* to *cis* photoisomerization of azobenzene on the vector induces the loosening of complexes; thus more DNA molecules escape from the condensates and finally enter the nuclei for transcription.

- 12 T. Hashimoto, Y. Tachibana, H. Nozaki, O. Mazda, T. Niidome, A. Murakami and T. Yamaoka, *Chem. Lett.*, 2009, **38**, 718.
- 13 F. Dai, P. Sun, Y. Liu and W. Liu, *Biomaterials*, 2010, **31**, 559.
- 14 A. Høgset, L. Prasmickaite, T. E. Tjelle and K. Berg, *Hum. Gene Ther.*, 2000, **11**, 869.
- 15 K. Berg, P. K. Selbo, L. Prasmickaite, T. E. Tjelle, K. Sandvig, J. Moan, G. Gaudernack, O. Fodstad, S. Kjolsrud, H. Anholt, G. H. Rodal, S. K. Rodal and A. Høgset, *Cancer Res.*, 1999, **59**, 1180.
- 16 L. Prasmickaite, A. Høgset, T. E. Tjelle, V. M. Olsen and K. Berg, *J. Gene Med.*, 2000, **2**, 477.
- 17 G. Han, C. C. You, B. J. Kim, R. S. Turingan, N. S. Forbes, C. T. Martin and V. M. Rotello, *Angew. Chem., Int. Ed.*, 2006, **45**, 3165.
- 18 T. Nagasaki, K. Wada and S. Tamagaki, *Chem. Lett.*, 2003, **32**, 88.
- 19 Z. Li, J. C. Barnes, A. Bosoy, J. F. Stoddart and J. I. Zink, *Chem. Soc. Rev.*, 2012, **41**, 2590.
- 20 N. G. Liu, D. R. Dunphy, P. Atanassov, S. D. Bunge, Z. Chen, G. P. López, T. J. Boyle and C. J. Brinker, *Nano Lett.*, 2004, **4**, 551.
- 21 J. Lu, E. Choi, F. Tamanoi and J. I. Zink, *Small*, 2008, **4**, 421.
- 22 C. Liu, P. Zhang, X. Zhai, F. Tian, W. Li, J. Yang, Y. Liu, H. Wang, W. Wang and W. Liu, *Biomaterials*, 2012, **33**, 3604.
- 23 P. Zhang and W. Liu, *Biomaterials*, 2010, **31**, 3087.
- 24 P. Zhang, J. Yang, W. Li, W. Wang, C. Liu, M. Griffith and W. Liu, *J. Mater. Chem.*, 2011, **21**, 7755.
- 25 Z. H. Wang, Y. Zhu, M. Y. Chai, W. T. Yang and F. J. Xu, *Biomaterials*, 2012, **33**, 1873.
- 26 H. Z. Jia, X. H. Luo, H. Cheng, J. Yang, C. Li, C. W. Liu, J. Feng, X. Z. Zhang and R. X. Zhuo, *J. Mater. Chem.*, 2012, **22**, 24092.
- 27 T. S. Lee, D. Y. Kim, X. L. Jiang, L. Li, J. Kumar and S. Tripathy, *Macromol. Chem. Phys.*, 1997, **198**, 2279.
- 28 F. Dai and W. Liu, *Biomaterials*, 2011, **32**, 628.
- 29 S. Ghosh and A. K. Banthia, *Tetrahedron Lett.*, 2001, **42**, 501.
- 30 M. Thomas and A. M. Klibanov, *Proc. Natl. Acad. Sci. U. S. A.*, 2002, **99**, 14640.
- 31 S. Osanai and K. Nakamura, *Biomaterials*, 2000, **21**, 867.
- 32 F. J. Pavinatto, A. Pavinatto, L. Caseli, D. S. dos Santos Jr, T. M. Nobre, M. E. D. Zaniquelli and O. N. Oliveira Jr, *Biomacromolecules*, 2007, **8**, 1633.
- 33 N. Fang, V. Chan, H. Q. Mao and K. W. Leong, *Biomacromolecules*, 2001, **2**, 1161.
- 34 D. J. Coady, Z. Y. Ong, P. S. Lee, S. Venkataraman, W. Chin, A. C. Engler, Y. Y. Yang and J. L. Hedrick, *Adv. Healthcare Mater.*, 2013, DOI: 10.1002/adhm.201300554.
- 35 R. Sarkar and S. K. Pal, *Biomacromolecules*, 2007, **8**, 3332.